J Mol Model (2012) 18:4577–4589
DOI 10.1007/s00894-012-1425-0

ORIGINAL PAPER

The assessment and application of an approach to noncovalent interactions: the energy decomposition analysis (EDA) in combination with DFT of revised dispersion correction (DFT-D3) with Slater-type orbital (STO) basis set

Wei Gao · Huajie Feng · Xiaopeng Xuan · Liuping Chen

Received: 1 January 2012 / Accepted: 3 April 2012 / Published online: 29 May 2012

Abstract An assessment study is presented about energy decomposition analysis (EDA) in combination with DFT including revised dispersion correction (DFT-D3) with Slater-type orbital (STO) basis set. There has been little knowledge about the performance of the EDA+DFT-D3 concerning STOs. In this assessment such an approach was applied to calculate noncovalent interaction energies and their corresponding components. Complexes in S22 set were used to evaluate the performance of EDA in conjunction with four representative types of GGA-functionals of DFT-D3 (BP86-D3, BLYP-D3, PBE-D3 and SSB-D3) with three STO basis sets ranging in complexity from DZP, TZ2P to QZ4P. The results showed that the approach of EDA+BLYP-D3/TZ2P has a better performance not only in terms of calculating noncovalent interaction energy quantitatively but also in analyzing corresponding energy components qualitatively. This approach (EDA+BLYP-D3/TZ2P) was thus applied further to two representative large-system complexes including porphine dimers and fullerene aggregates to gain a better insight into binding characteristics.

Keywords Assessment · DFT-D3 · EDA · Noncovalent interaction · STO

W. Gao · H. Feng · L. Chen (✉)
KLGHEI of Environment and Energy Chemistry,
School of Chemistry and Chemical Engineering,
Sun Yat-sen University,
Guangzhou 510275, China
e-mail: cesclp@mail.sysu.edu.cn

W. Gao
College of Pharmacy, Guangdong Pharmaceutical University,
Guangzhou 510006, China

X. Xuan
School of Chemical and Environmental Sciences,
Key Laboratory of Green Chemical Media and Reactions,
Ministry of Education, Henan Normal University,
Xinxiang, Henan 453007, China

Introduction

Noncovalent interaction is ubiquitous in a wide variety of chemical [1], physical [2], and biological processes [3]. It is the main origin of stability for many cases from gas to liquid and solid. Examples include, but are certainly not limited to, solvation, ionic liquid, crystallization, asymmetric catalysis, bulk-phase properties, self-assembly of various size supramolecular, nanomaterials, chromatographic separation, micelle formation, molecular recognition, as well as the structure and function of biomolecules from simple peptides to enzymes and DNA. There are many types of noncovalent interactions including hydrogen bond, halogen bond, van der Waals contact, π-π, etc. However, with respect to these different intermolecular interactions, their strength and nature would be quite different.

Conventionally, the term "noncovalent interaction" is used here to encompass contributions from electrostatic, induced dipole, dispersion energy, etc. In investigations of noncovalent interactions the supermolecular *ab initio* calculations have become very popular tools. The total noncovalent interaction

energy ΔE can be readily computed from the complex and fragments as:

$$\Delta E = E(AB) - E(A) - E(B). \quad (1)$$

Nevertheless, it is often desirable to obtain a reasonable and clear description of the component interaction energies contributing to the total noncovalent interaction energy when we need a deeper insight into the physical nature of this interaction. To achieve this goal, a variety of interaction energy decomposition schemes have been proposed [4–18], most of which fall into two categories, namely, the perturbation methods [11–15] and supermolecular methods [16–18]. The former is represented by symmetry-adapted perturbation theory (SAPT) while the latter by extended transition state (ETS).

In the usual SAPT method, the interaction energy can be expressed as:

$$\Delta E = E^{(1)}_{\mathrm{elstat}} + E^{(2)}_{\mathrm{disp}} + E^{(2)}_{\mathrm{ind}} + E^{(1)}_{\mathrm{exch}} + E^{(2)}_{\mathrm{exch-ind}} + E^{(2)}_{\mathrm{exch-disp}} + \Delta^{(3-\infty)}. \quad (2)$$

Here, $E^{(1)}_{\mathrm{elstat}}$ is the electrostatic interaction energy derived from the electron densities of the monomers; $E^{(2)}_{\mathrm{disp}}$ is the dispersion interaction energy required the frequency-dependent response propagators of the two monomers; and $E^{(2)}_{\mathrm{ind}}$ is the induction interaction energy described by static response propagators of the monomers. These terms are accompanied by the additional exchange terms $E^{(1)}_{\mathrm{exch}}$, $E^{(2)}_{\mathrm{exch-ind}}$ and $E^{(2)}_{\mathrm{exch-disp}}$, which arise due to the tunnelings of the electrons from one monomer to the other if the electron densities of the monomer overlap with each other. In SAPT practical scheme, the third- or higher order contributions are usually not to be calculated [19].

Another energy decomposition scheme based on the supermolecular method can be performed more easily. This method was initially proposed by Kitaura-Morokuma [16, 17] and later developed by Ziegler-Rauk [18] and now is conventionally referred to as energy decomposition analysis (EDA), which has turned out to be extremely useful for treating noncovalent interactions. In this scheme, the total interaction energy ΔE_{int} is decomposed into a number of physically meaningful components (if the dispersion term is considered):

$$\Delta E_{\mathrm{int}} = \Delta E_{\mathrm{elstat}} + \Delta E_{\mathrm{pauli}} + \Delta E_{\mathrm{orb}} + \Delta E_{\mathrm{disp}}. \quad (3)$$

Here, $\Delta E_{\mathrm{elstat}}$ gives the electrostatic interaction energy between the fragments calculated with the electron density distribution in the complex. $\Delta E_{\mathrm{pauli}}$ denotes the repulsive interactions between the fragments which are caused by the fact that two electrons with the same spin cannot occupy the same region in space. ΔE_{orb} accounts for the stabilizing orbital interaction energy as a result of the inter-atomic orbital overlapping. ΔE_{disp} measures the dispersion energy of intermolecules. An essential advantage of the EDA method is that it provides a complete energy description of a complex, not only the intermolecular interaction but also intra-molecular interaction which is unable to be treated by the SAPT approach. Therefore, we believe EDA to be a good and promising method for data collection and analysis.

From (2) and (3) it can be seen that some different energy components are defined in the perturbation methods and supermolecular methods. However, it should be noted that in different methods determining which energy components to use is somewhat arbitrary and without rigorous physical basis. And there is no agreement between different methods on which components should be considered, not to mention comparisons of values of corresponding energy components. Moreover, the energy components of noncovalent interactions, even if calculated with highest accurate methods, have not yet been supported by generally accepted experimentation, which remains challenging to future work. In light of this, our interest focuses on the qualitative analysis of energy components, rather than quantitative.

When it comes to accurate calculations of intermolecular interaction energies, we have two issues to consider. On the one hand, whether the result of total interaction energy is accurate strongly depends on the method used to describe molecular interaction. Many previous works made use of expensive calculation methods with large basis sets to provide accurate noncovalent interaction energies [20–26]. There is a high computational demand and it is time consuming. For example, the CPU time for the CCSD(T) calculation, which is recognized as the "golden standard", is proportional to the 7th power of the number of basis functions, while the CPU time for the MP2 calculation, which is often used for the evaluation of intermolecular interaction energies, is proportional to the 5th power of the number of basis functions. Unfortunately, the MP2 method overestimates the attraction in the aromatic clusters compared to more reliable calculations [26]. These facts mean the application of expensive calculation methods to large systems becomes computationally prohibitive. Density functional theory (DFT), which is widely used in quantum mechanical (QM) calculations for its low computational cost, is often inadequate in describing noncovalent interaction energies because it fails to treat dispersion effects completely. Nevertheless, the DFT community has recently developed a variety of methods for the treatment of van der Waals (dispersion) interactions, including treatments with i) specialized functionals, such as M05/M06 series [27, 28], ii) semiempirically dispersion corrected functionals, such as B97D [29], iii) dispersion corrected atom centered pseudopotentials within the framework of KS-DFT, such as DCACP [30], and iv) double hybrid functionals, such as B2PLYP [31]. Among these DFT approaches, the semiempirical dispersion corrected functionals (DFT-D) approach has been developed [26, 29, 32–34] by adding an empirical dispersion corrected

term, which proves to be an efficient way to describe dispersion effects. A large number of dispersion corrected terms have been developed for the treatment of noncovalent interactions, each term specifically for different functionals, like PBE-D, B3LYP-D etc. Very recently, the revised DFT-D method (DFT-D3) [33, 34] was proposed as a more improved tool to compute the dispersion energy due to its higher accuracy, broader range of applicability, and less empiricism.

On the other hand, accurate computations of noncovalent interactions also require very large basis sets [24–26, 35, 36]. This is not surprising because dispersion interactions can be expressed in terms of the polarizabilities of the weak interacting molecules, and polarizability computations are known to require large basis sets. In order to test the effect of the Slater-type orbitals (STOs) basis set [37, 38], we ran DFT-D3 calculations, using the STO basis sets available in ADF software, from the medium DZP (double-ξ, with one polarization functions) up to very large QZ4P (quadruple-ξ with four polarization functions). In QM calculations, to obtain the same level of accuracy, one is often likely to use a smaller number of STOs than Gaussian-type orbitals (GTOs) [39] because of the right asymptotic form and correct nuclear cusp behavior.

To sum up, it is interesting and convenient for us to take the approach of EDA in combination with the DFT-D3 with STO basis sets to study the noncovalent interaction energy and their energy components.

There are numerous assessment investigations [24, 33, 35, 40–48] about calculating noncovalent interaction energy by various QM theoretical methods with various basis sets. Given the rapid development of new DFT-D methods over the past years, several functionals emerged as "best performances" to treat noncovalent interactions. After an extensive and careful review, Riley and co-workers reported that B97-D and ωB97X-D are currently the most recommendable DFT-based methods for noncovalent interaction energy [24]. A contrasting accord was reached by Grimme et al., who compared old (DFT-D2) and new (DFT-D3) variants of 11 functionals beyond the effects of BSSE for bioorganic molecules, and they concluded that B2PLYP-D is best overall [33, 34]; While Sherill et al. thought that the B2PLYP-D3, B3LYP-D3, B97-D3 and PBE-D3 methods perform well in treating noncovalent interaction energy [35]. The latest and the most thorough assessment was performed by Grimme on new GMTKN30 database, which concluded that DSD-BLYP-D3 was the best functional on the quadruple-ξ level and closely followed by PWPB95-D3 [42].

However, despite these above-mentioned assessments, it might be noted that almost all of the calculating methods of noncovalent interaction energy were based on the supermolecular QM approaches as Eq. (1). To the best of our knowledge, although the approach of EDA+DFT-D has been devoted to a few investigations [41, 42, 49], still no detailed assessments combining EDA and DFT-D3 have been reported, especially with various DFT-D3 functionals with different STO types of basis sets. As is well known, with the same accuracy requirement and the same calculating methods, the number of STOs is generally smaller than that of GTOs basis set [39]. Consequently, using STOs basis set instead of GTOs may improve efficiency in practical QM calculation.

Therefore, the assessment of the approach of EDA+DFT-D3/STOs would be of interest for further investigation. In this paper, we evaluated the performance of EDA method with four different but representative types of GGA-functionals of DFT-D3 (BP86-D3, BLYP-D3, PBE-D3 and SSB-D3) with three STO basis sets (DZP, TZ2P, QZ4P) against the benchmark set S22. Note that the assessment of GGA-functionals of DFT-D3 is particularly useful because most popular QM softwares support these types of functionals and a vast amount of chemistry has been handled by GGA-functionals calculations. The results of this assessment should be useful in accurate computations of noncovalent interactions, not only in terms of accuracy but also of computational cost, which is of particular interest for large supramolecular systems. Furthermore, it can help us gain a deeper insight into the nature of the noncovalent interaction by analysis of the physically meaningful energy components resulted from EDA+DFT-D3. To demonstrate the advantage of this approach of EDA+DFT-D3, on the basis of the assessment results, we further applied this approach to two representative large-system examples of porphine dimers and fullerene aggregates.

Methods

We choose the S22 database as test set. S22 set is a key and most popular database provided by Hobza and co-workers [20], which contains 22 dimers of various types (hydrogen bond, dispersion dominated and mixed). Table 1 lists their detailed information about dimers which consists of small to medium-sized (30 atoms) complexes of common molecules containing C, N, O, and H, with single, double, and triple bonds. Moreover, S22 database consists of high-accuracy geometries and their CCSD(T)/CBS interaction energies.

As previously discussed, to evaluate the noncovalent interaction energy of complexes, we adopted the EDA method proposed by Kitaura–Morokuma and developed by Ziegler–Rauk [16–18], combined with four GGA-levels DFT-D3 functionals at three basis sets. Specifically, this approach follows three steps to integrate dispersion energy into density functionals: i) EDA with DFT functionals is implemented with ADF 2012.01 [50] without particular regard for dispersion correction, and three components can be obtained: the electrostatic $\Delta E_{\mathrm{elstat}}$, the pauli repulsion $\Delta E_{\mathrm{pauli}}$ and the orbital interaction ΔE_{orb}. ii) The dispersion correction term coupling with their corresponding DFT functionals are calculated respectively with program dftd3 available on Grimme's website [33, 34], and the dispersion energy ΔE_{disp} can be obtained.

Table 1 Energy components contribution to total noncovalent interaction energy ΔE_{int} from EDA (BLYP-D/TZ2P) and total noncovalent interaction energy $\Delta E_{ccsd(T)}$ from CCSD(T)/CBS for the different types of complexes (all data in kcal mol^{-1})

	ΔE_{int} [a]	ΔE_{disp}	ΔE_{elstat}	ΔE_{orb}	ΔE_{pauli}	$\Delta E_{ccsd(T)}$ [b]
	Hydrogen bonded complexes					
$(NH_3)_2$	−3.01	−1.08	−4.93	−1.70	4.70	−3.17
$(H_2O)_2$	−5.08	−0.78	−7.85	−3.85	7.40	−5.02
formic acid dimer	−19.39	−3.00	−31.96	−25.56	41.13	−18.61
formamide dimer	−16.23	−3.10	−24.72	−15.51	27.10	−15.96
uracil dimer	−20.84	−4.03	−29.38	−18.46	31.03	−20.65
2-pyridoxine·2-aminopyridine	−17.96	−4.78	−27.84	−17.07	31.73	−16.71
adenine· thymine WC	−17.21	−5.11	−27.38	−16.30	31.58	−16.37
	Dispersion dominated complexes					
$(CH_4)_2$	−0.51	−1.03	−0.17	−0.22	0.91	−0.53
$(C_2H_4)_2$	−1.43	−2.43	−1.10	−0.63	2.73	−1.51
benzene· CH_4	−1.53	−2.60	−1.21	−0.71	2.99	−1.50
PD benzene dimer	−3.55	−7.94	−3.51	−1.26	9.16	−2.73
pyrazine dimer	−4.97	−8.14	−4.68	−1.97	9.82	−4.42
uracil dimer	−10.45	−11.05	−9.06	−2.94	12.60	−10.12
stacked indole·benzene	−5.67	−11.27	−5.75	−2.05	13.40	−5.22
stacked adenine· thymine	−12.14	−15.53	−11.50	−4.17	19.06	−12.23
	Mixed complexes					
ethene·ethyne	−1.74	−1.22	−1.60	−1.11	2.19	−1.53
benzene·H_2O	−3.21	−2.58	−2.15	−1.83	3.35	−3.28
benzene·NH_3	−2.31	−2.64	−1.50	−1.14	2.97	−2.35
benzene·HCN	−4.48	−3.42	−2.81	−2.91	4.66	−4.46
T-shaped benzene dimer	−2.87	−4.41	−1.97	−1.39	4.90	−2.74
T-shaped indole·benzene	−5.57	−5.97	−3.66	−3.09	7.15	−5.73
phenol dimer	−6.97	−4.84	−8.60	−4.96	11.43	−7.05

a) $\Delta E_{int} = \Delta E_{elstat} + \Delta E_{pauli} + \Delta E_{orb} + \Delta E_{disp}$; ΔE_{disp} and ΔE_{int} have only three significant digits to be showed here

b) $\Delta E_{ccsd(T)}$ calculated at CCSD(T)/CBS from ref [20]

Note the damping function uses BJ-damping scheme instead of zero-damping because DFT-D3 (BJ) is on average slightly better than DFT-D3 (zero) for typical noncovalent interactions [51]. iii) Combining results i) and ii) into total interaction energy, and the result is expressed by Eq. (3). Therefore, the interaction energies and their corresponding components of physical meaning are calculated completely for each complex at each level of theory. As we have noticed, while this article was being written up, some usual DFT-D3 functionals are already supported by the latest version of ADF package. Nevertheless, our procedure is more flexible with controls and can provide more details about dispersion energy.

The performance of the approach (EDA+DFT-D3) for a given test set is evaluated by comparing the interaction energy of each complex with that of its reference CCSD (T)/CBS value, as:

$$x_{ref} = \left(x_{DFT-D3} - x_{CCSD(T)/CBS}\right)/x_{CCSD(T)/CBS}. \quad (4)$$

A most popular measure of these relative errors is denoted as mean absolute error (MAE) and is expressed as:

$$\mathrm{MAE} = \frac{1}{n}\sum_{ref}^{n}\left|x_{ref}\right|, \quad (5)$$

where $|x_{ref}|$ is the absolute value of results from (4) and n means the total quantity of complexes in subgroups (i.e., hydrogen bond, dispersion dominated, mixed) of test sets.

On the other hand, among these energy components, the ΔE_{disp} and ΔE_{elstat} are particularly important because they are commonly employed in various energy decomposition schemes and moreover, they are applied to determination of the dimer types. To check whether the energy components calculated by different combinations (EDA of DFT-D3 and STOs) are reasonable or not, the ratios of $\Delta E_{disp}/\Delta E_{int}$ and $\Delta E_{elstat}/\Delta E_{int}$ are plotted and compared (see Figs. 1, 2, 3). Here, instead of using ΔE_{disp} and ΔE_{elstat}, the ratios of $\Delta E_{disp}/\Delta E_{int}$ and $\Delta E_{elstat}/\Delta E_{int}$ are used to eliminate the magnitude difference of dispersion and electrostatic energy

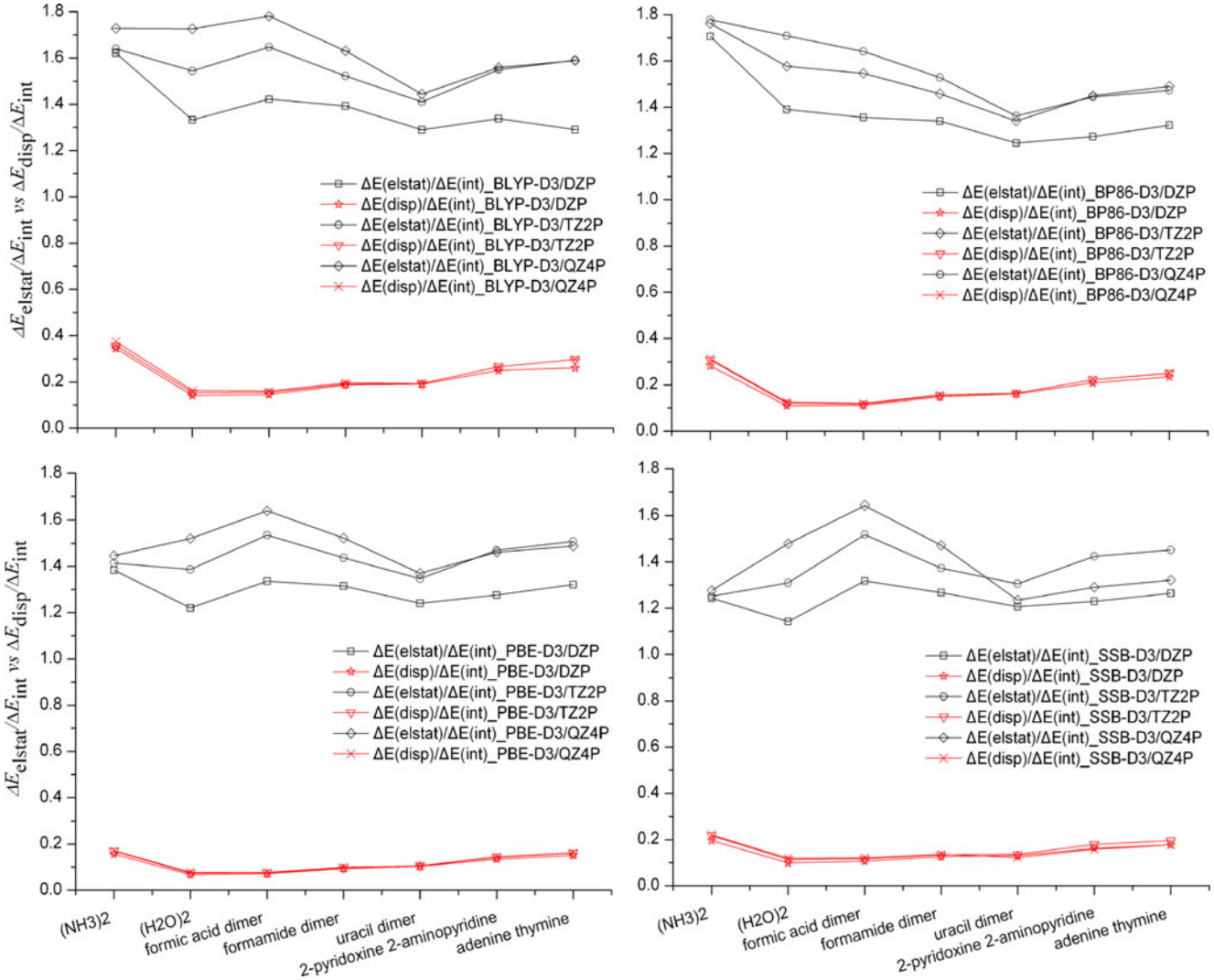

Fig. 1 Comparisons of ratios of dispersion energy $\Delta E_{disp}/\Delta E_{int}$ and electrostatic energy $\Delta E_{elstat}/\Delta E_{int}$ for hydrogen bond subset from EDA with the different GGA-functionals of DFT-D3 at different STO basis sets. The X-axis coordinate represented a series of complexes in hydrogen bond subset in S22. For more details see Table 1

calculated for various dimers with different strengths of noncovalent interaction. Next, a reasonable assessment of ΔE_{disp} and ΔE_{elstat} is performed. As we know, a total of 22 complexes in S22 set are divided into three subgroups, which is generally accepted: seven hydrogen bond complexes predominantly by electrostatic interactions, eight complexes predominantly by dispersion interactions and seven complexes in which the contribution of electrostatic and dispersion interactions are considered to be similar. For example, in the NH_3 dimer, ΔE_{disp} is qualitatively not important and the total interaction energy is dominated by ΔE_{elstat}, which is a characteristic of a hydrogen bond complex. The C_2H_4 dimer represents the other extreme where the interaction energy asymptotically is given by ΔE_{disp} while ΔE_{elstat} is smaller, which is a feature of a complex of dispersion dominated characteristic. So, it can be qualitatively estimated that whether ΔE_{elstat} and ΔE_{disp} calculated by different combinations (EDA of DFT-D3 and STOs) are located in reasonable range. We believe that both dispersion and electrostatic contribution resulted from appropriate combinations of DFT-D3 functionals with STO basis sets would be restricted within the reasonable range, and will lead to correct classifications of types of complexes by ΔE_{elstat} and ΔE_{disp}; while inappropriate combinations may seriously deviate either ΔE_{elstat} or ΔE_{disp} from the reasonable range and may lead to wrong classifications. Consequently, the match between the generally-accepted classifications against S22 set and our classifications determined by varying dominant energy resulted from different EDA+DFT-D3/STOs was made.

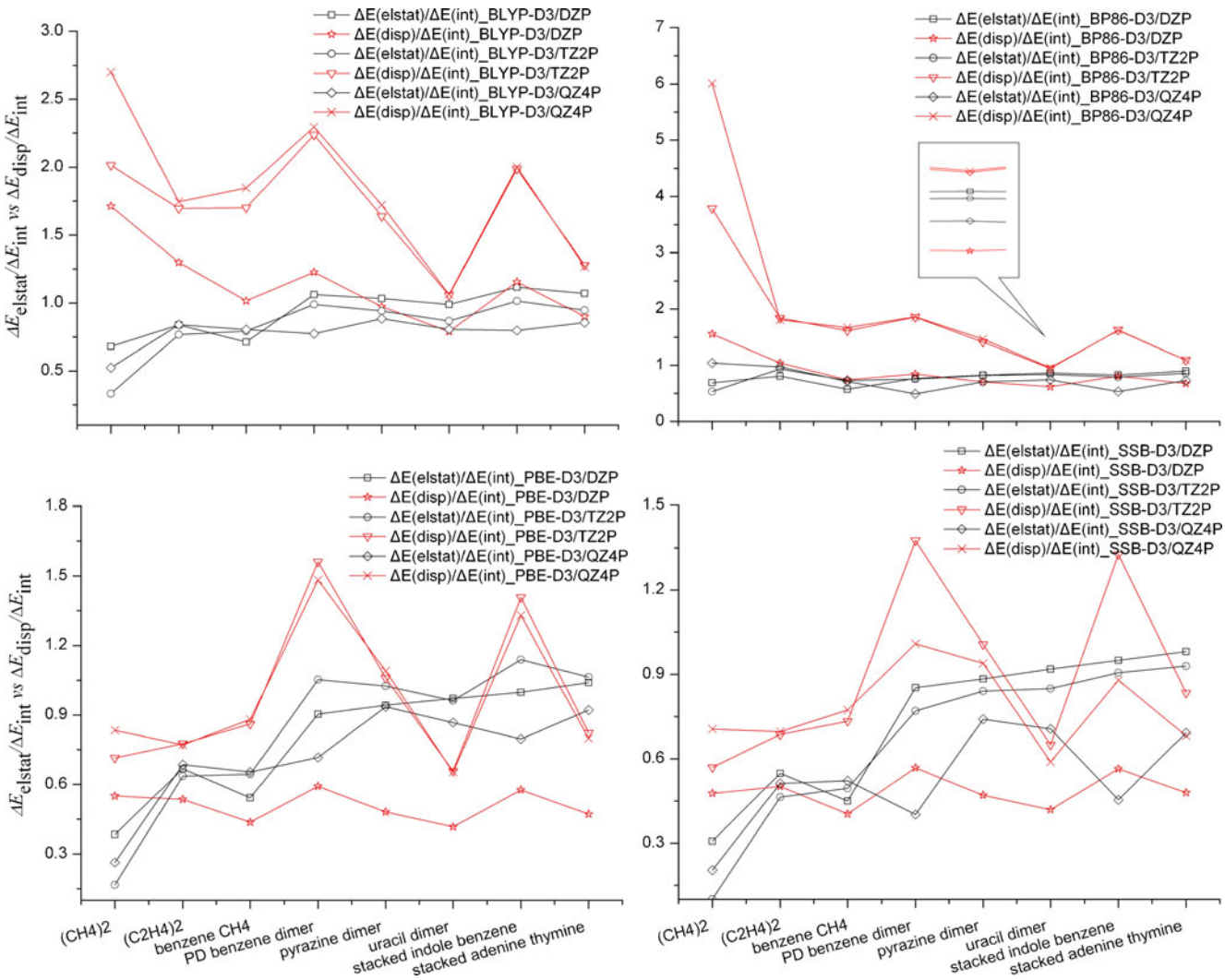

Fig. 2 Comparison of ratios of dispersion energy $\Delta E_{disp}/\Delta E_{int}$ and electrostatic energy $\Delta E_{elstat}/\Delta E_{int}$ for dispersion dominated subset from EDA with the different GGA-functionals of DFT-D3 at different STO basis sets. The X-axis coordinate represented a series of complexes in dispersion dominated subset in S22. For more details see Table 1

Results and discussion

The object of this paper is two fold. The first purpose of this study, a benchmarked one in quantity, is to assess the accuracy of this approach to predict noncovalent interaction energy, that is, to study how the GGA-functionals including dispersion correction with different STO basis sets influence the results of the total interaction energy calculated by EDA methods. A comprehensive list of total interaction and each energy component for S22 set are available in Table 1, which are calculated by EDA+BLYP-D3/TZ2P. Details of other GGA-functionals results are not listed but their MAEs are collected in Table 2.

The second goal is to assess in quality the match between the generally-accepted classifications and our classifications by using the ratio of $\Delta E_{disp}/\Delta E_{int}$ and $\Delta E_{elstat}/\Delta E_{int}$. However, as we have pointed out, so far there has been no accurate value of energy components calculated by theoretical methods and validated by experiment results. Thus, we use the term *reasonable* instead of *accurate* in discussion of energy components. Based on the achievement of these two goals, we can comprehensively understand the performance of EDA+DFT-D3/STOs and find the best combination of this method.

Hydrogen bond complexes

Now, let us discuss the total noncovalent interaction energies from EDA+DFT-D3 results compared with those from CCSD(T)/CBS. With the DZP basis set, all four DFT-D3 severely overestimate the interaction energies by MAE>0.1 or close to 0.1, which indicate these methods fail to describe the hydrogen bond interaction at this basis set level. With

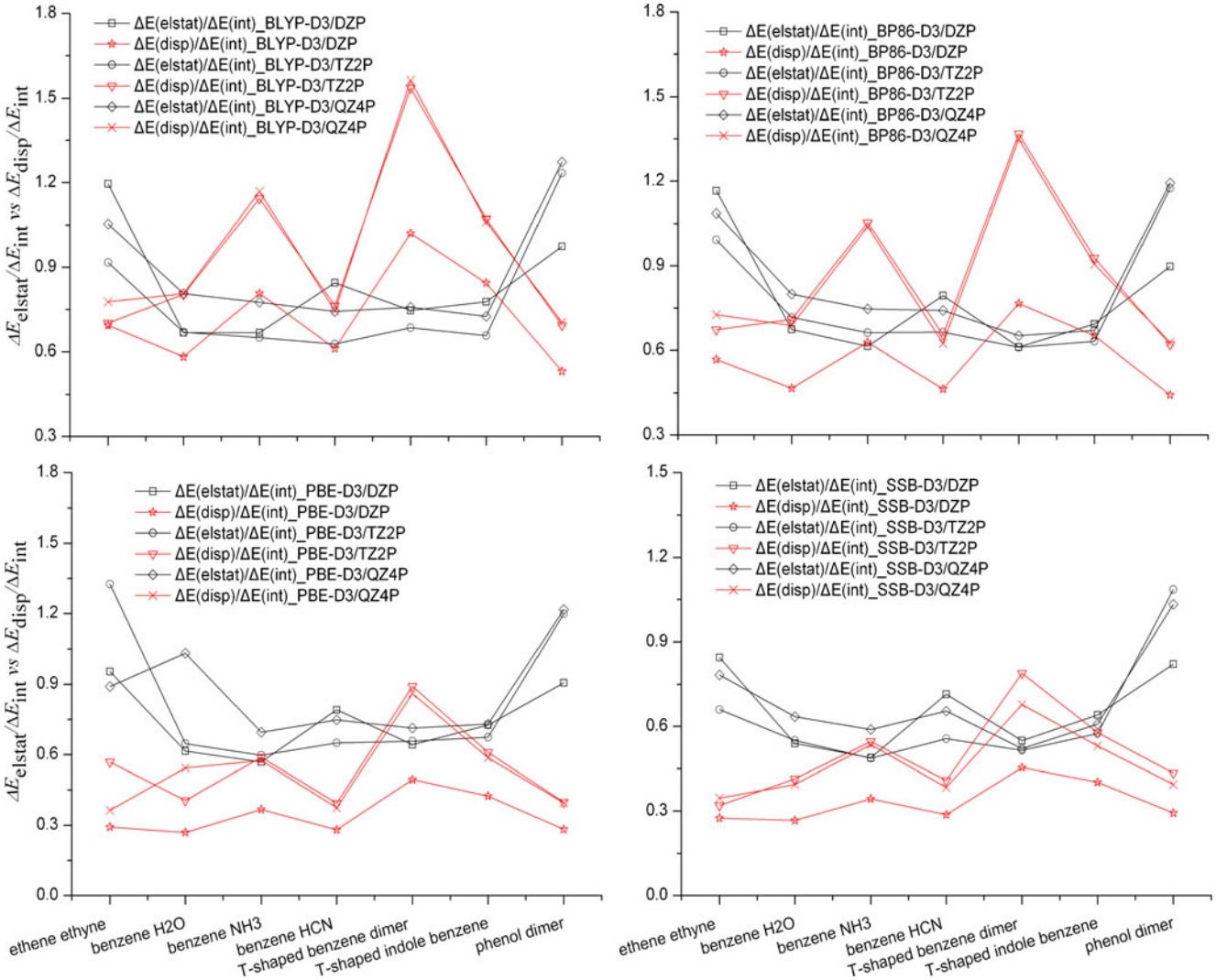

Fig. 3 Comparison of ratios of dispersion energy $\Delta E_{disp}/\Delta E_{int}$ and electrostatic energy $\Delta E_{elstat}/\Delta E_{int}$ for mixed subset from EDA with the different GGA-functionals of DFT-D3 at different STO basis sets. The X-axis coordinate represented a series of complexes in mixed subset in S22. For more details see Table 1

the TZ2P and QZ4P basis set, BLYP-D3 seems to have a better performance (MAE<0.05) than those of the BP86-D3, PBE-D3 and SSB-D3 in predicting interaction energy. However, the latter three DFT-D3 are sufficient to estimate the energy for hydrogen bond complexes in which MAE< or ≈0.1. Note the MAEs change marginally with the increase of basis set size from TZ2P to QZ4P, whereas the MAE for SSB-D3 even increases when the basis set size is increased from TZ2P to QZ4P. This observation gives us confidence to conclude that BLYP-D3 with the TZ2P or QZ4P basis set can provide reliable results. Certainly, more costly computation is required for QZ4P basis set level.

Next, it can be readily seen from Fig. 1, that in each hydrogen bond complex, the electrostatic ratio $\Delta E_{elstat}/\Delta E_{int}$ is much larger than the dispersion one $\Delta E_{disp}/\Delta E_{int}$, indicating that the former dominates over the latter. The results are consistent with the description of complexes of hydrogen bond type in the above discussion (i.e., $\Delta E_{elstat}>\Delta E_{disp}$). The ratios of $\Delta E_{elstat}/\Delta E_{int}$ and $\Delta E_{disp}/\Delta E_{int}$ are relatively reasonable by these four DFT-D3 methods (BLYP-D3, BP86-D3, PBE-D3 and SSB-D3) with three STO basis sets. The results are favorable mainly because ΔE_{elstat} is far larger than the ΔE_{disp} in hydrogen bond complex. In addition, the data points of $\Delta E_{disp}/\Delta E_{int}$ at the different STO levels overlap because they are close to each other, as shown in Fig. 1.

Considering the above results from both ΔE_{int} and $\Delta E_{elstat}/\Delta E_{int}$, $\Delta E_{disp}/\Delta E_{int}$, we hold that all four functionals EDA+DFT-D3 at TZ2P or QZ4P are sufficient to calculate satisfactorily noncovalent interaction energies and their energy components of hydrogen bond complex.

Table 2 Comparison of MAEs for the S22 benchmark set and its subset by EDA with the different GGA-functionals of DFT-D3 at different STO basis set; along with the results from S22+ set by SAPT-DFT/ aug-cc-pVTZ

		DZP	TZ2P	QZ4P	aug-cc-pVTZ
BLYP-D3	Hydrogen bond	0.090	0.037	0.041	
	Dispersion dominated	0.625	0.081	0.108	
	Mixed	0.321	0.039	0.028	
	Overall	1.036	0.157	0.177	
PBE-D3	Hydrogen bond	0.154	0.085	0.074	
	Dispersion dominated	0.971	0.168	0.138	
	Mixed	0.569	0.068	0.105	
	Overall	1.694	0.321	0.317	
BP86-D3	Hydrogen bond	0.107	0.075	0.076	
	Dispersion dominated	1.009	0.233	0.250	
	Mixed	0.507	0.042	0.045	
	overall	1.623	0.350	0.371	
SSB-D3	Hydrogen bond	0.183	0.079	0.117	
	Dispersion dominated	1.139	0.298	0.323	
	Mixed	0.802	0.063	0.288	
	Overall	2.124	0.440	0.728	
SAPT-DFT[a)]	Hydrogen bond				0.034
	Dispersion dominated				0.058
	Mixed				0.057
	Overall				0.149

a) The results of SAPT-DFT/ aug-cc-pVTZ and corresponding CCSD(T)/CBS (equilibrium geometry dimers in S22+) are provided by Hesselmann [19], but do not include the large complexes of pyrazine dimer and 2-pyridoxine·2-aminopyridine

Dispersion dominated complexes

As can be seen from Table 2, with DZP basis set, the EDA with the four DFT-D3 methods (BLYP-D3, BP86-D3, PBE-D3 and SSB-D3) fails to qualify the interaction energy of the dispersion dominated complexes. While with the basis sets of TZ2P and QZ4P, the MAEs of the PBE-D3, BP86-D3 and SSB-D3 methods are large (>0.10), and their order of increase of MAEs is the following as PBE-D3<BP86-D3<SSB-D3. These data suggest that the functionals/basis sets mentioned above might be inappropriate for calculating complexes involving predominated dispersion. Fortunately, the much better performances of BLYP-D3 with TZ2P and QZ4P are evidently seen such that MAEs are found respectively to be≈0.08 and≈0.10, both errors being roughly equal or slightly smaller by about 10 %. Interestingly, increasing the basis set results in larger errors for the dispersion dominated complexes than those for the hydrogen bond complexes. This is perhaps not surprising in that polarizability (to which dispersion is related) is known to be difficult to converge with respect to basis set. Thus, the increasing complexity of basis set does not necessarily bring more accurate results for noncovalent interaction.

Secondly, when we consider complexes dominated by dispersion, the first glance at Fig. 2 informs that the difference between $\Delta E_{elstat}/\Delta E_{int}$ and $\Delta E_{disp}/\Delta E_{int}$ is not clearer than hydrogen bond complexes. This is because the dispersion term is merely slightly larger than electrostatic term in the complexes predominated by dispersion. i) As shown in Fig. 2, calculated by all four DFT-D3 calculated at DZP basis set, most data points of $\Delta E_{disp}/\Delta E_{int}$ are located below or near those of $\Delta E_{elstat}/\Delta E_{int}$, which indicates the ΔE_{elstat} term is larger than or almost equal to ΔE_{disp}. The results suggest these methods with DZP basis set fail to agree on the features in these complexes (i.e., $\Delta E_{disp}>\Delta E_{elstat}$). ii) Both the BLYP-D3 and BP86-D3 with TZ2P or QZ4P have illustrated that data points of $\Delta E_{elstat}/\Delta E_{int}$ are below data points of $\Delta E_{disp}/\Delta E_{int}$ from Fig. 2. They show a quite satisfactory distinctive results for complexes dominated by dispersion. iii) When the basis set size is increased to TZ2P and QZ4P level, PBE-D3 and SSB-D3 methods perform a bit worse than BLYP-D3 and BP86-D3 because two wrong data points where $\Delta E_{disp}/\Delta E_{int}$ is smaller than $\Delta E_{elstat}/\Delta E_{int}$ are observed. Therefore, there is convincing evidence that BLYP-D3 and BP86-D3 with TZ2P or QZ4P are more reasonable than PBE-D3 and SSB-D3 with TZ2P or QZ4P in analysis of ΔE_{disp} and ΔE_{elstat} qualitatively for dispersion dominated complexes. And EDA+BLYP-D3/ TZ2P is sufficient either in terms of predicting total interaction energy quantitatively or analyzing corresponding energy components qualitatively.

Mixed complexes

Firstly, for all four DFT-D3 with DZP basis set that we have tested, there is a remarkable failure to calculate the interaction energy for mixed complexes because of the poor prediction of both hydrogen bond and dispersion dominated interactions.

On the contrary, BLYP-D3 at TZVP/QZ4P does well for prediction of interaction energies in the mixed complexes, since it gives balanced high accuracy for hydrogen bond and dispersion dominated interactions. Somewhat to our surprise, the MAEs of the BP86-D3 with TZ2P or QZ4P for mixed complexes are less than those for dispersion dominated complexes and even those for hydrogen bond complexes. Also, PBE-D3 and SSB-D3 with TZ2P behave similarly and obtain rather successful results compared with those of CCSD(T)/CBS. These interesting results are actually not due to the methods of BP86-D3, PBE-D3 and SSB-D3 for adequate treatment of dispersion or electrostatic term for mixed complexes, but rather due to calculating errors of their two terms being counteracted in these methods. Another reason might be due to a compensation of errors, that is to say, a good balance comes from favorable cancellation of errors between the basis set and the theoretical approach (e.g., electron correlation and dispersion term). Both factors may act simultaneously, hence leading to an eventually significant error decrease.

Secondly, in mixed types of complexes, no reliable regularity can be given as to which should have a bigger value between ΔE_{elstat} and ΔE_{disp}. Therefore, we will not discuss this point like we have done in the two previous cases. For the result of this EDA+DFT-D3 approach also see Fig. 3.

Comparison of accuracy between basis sets of STO and GTO

Since the small STO basis set DZP tends to show very big errors for intermolecular energies, only STO basis sets of TZ2P and QZ4P are discussed here. Table 3 summarizes the mean absolute deviation (MAD) of noncovalent interaction energy between the approach of EDA+DFT-D3 with STO basis set and that of supermolecular-method+DFT-D3 with GTO basis set. The latter approach based on Eq. (1) is a general and popular way to calculate the noncovalent interaction energy. In Table 3, the MADs from EDA+BLYP-D3 with TZ2P and QZ4P indicate slightly bigger errors than those from supermolecular-method+BLYP-D3 with def2-QZVP in ref [33]. Considering the large gain in computational efficiency for STO basis set, the error from EDA+BLYP-D3 is entirely acceptable. Meanwhile, it also suggests that EDA+BLYP-D3/TZ2P can be considered as a good choice for the study of noncovalent interactions and can be expected with reasonably accurate results. Overall, the EDA+BP86-D3 and supermolecular-method+BP86-D3 show similar performance, with MADs of 0.61 (TZ2P), 0.59 (QZ4P) and 0.62 (def2-QZVP) kcal mol^{-1}, respectively. Also, the EDA+PBE-D3 and supermolecular-method+PBE-D3 yield similar errors, with MADs of 0.61 (TZ2P), 0.60 (QZ4P) and 0.62 (def2-QZVP) kcal mol^{-1}, respectively. However, both BP86-D3 and PBE-D3 have the bigger errors (>0.5 kcal mol^{-1}) and are somewhat unacceptable. By the way, EDA+SSB-D3 also shows bigger errors, especially with QZ4P basis set.

It is well recognized that the EDA+DFT-D3 with STO basis set (TZ2P or QZ4P) are sufficient to provide similar accurate results relative to supermolecular-method+DFT-D3 with very large GTO basis set def2-QZVP.

Table 3 Mean absolute deviations (MADs) between the approach of EDA+DFT-D3 in conjunction with STO basis set and the approach of supermolecular-method+DFT-D3 in conjunction with GTO basis set. [a,b]

	STO		GTO
	TZ2P	QZ4P	def2-QZVP
BLYP-D3	0.30	0.27	0.23
BP86-D3	0.61	0.59	0.62
PBE-D3	0.61	0.60	0.62
SSB-D3	0.68	1.12	

a) All values are in kcal mol^{-1} and based on the S22 benchmark set

b) MADs of supermolecular-method+DFT-D3 with def2-QZVP basis set from ref [33]

Comparison of EDA+BLYP-D3/TZ2P(QZ2P) with SAPT-DFT/aug-cc-pVTZ

We choose the results of EDA+BLYP-D3/TZ2P to compare with the latest results for equilibrium geometry dimers in S22+ set of SAPT-DFT/aug-cc-pVTZ provided by Hesselmann [19]. The SAPT-DFT calculations were done using the localized and asymptotically corrected LPBE0AC exchange correlation potential for the monomer calculations and Becke97 (B97) hybrid xc functional for the supermolecular calculations. It is useful to make a comparison of EDA methods with more familiar SAPT-DFT methods in order to assess their performance. From Table 2, SAPT reproduces fairly well the ΔE_{int} by CCSD(T)/CBS. On all and subsets, the errors for those at the SAPT-DFT/aug-cc-pVTZ level are slightly smaller than those at the BLYP-D3/TZ2P and BLYP-D3/QZ4P levels except for mixed subset.

With regard to the energy component analysis [19, 52], the ratios of energy component $\Delta E_{\text{elstat}}/\Delta E_{\text{int}}$ and $\Delta E_{\text{disp}}/\Delta E_{\text{int}}$ from the EDA+BLYP-D3/TZ2P (QZ4P) for complexes in S22 have a similar trend to those from the SAPT-DFT/aug-cc-pVTZ (see Fig. 4), which support that the EDA+BLYP-D3/TZ2P(QZ4P) can also produce reasonable evaluation of energy component for noncovalent dimers. By the way, note that the dispersion energy is calculated by $\Delta E_{\text{disp}} = E^{(2)}_{\text{disp}} + E^{(2)}_{\text{exch-disp}}$ from SAPT-DFT results.

Summary of assessment results

Through comparison with available CCSD(T)/CBS benchmarks of S22 set, the performance of EDA in combination with the four GGA-type DFT-D3 at three STO basis sets are

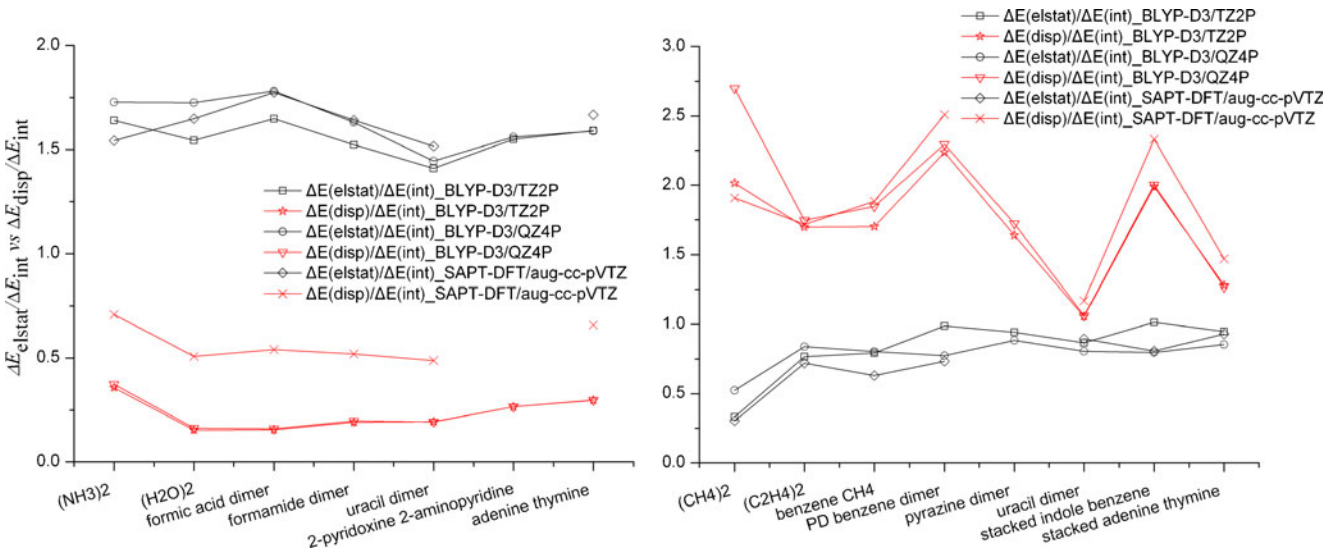

Fig. 4 Comparison of ratios of dispersion energy $\Delta E_{disp}/\Delta E_{int}$ and electrostatic energy $\Delta E_{elstat}/\Delta E_{int}$ by EDA+BLYP-D3/TZ2P(QZ2P) with those of SAPT-DFT/aug-cc-pVTZ for hydrogen bond subset as well as dispersion dominated subset. The results of SAPT-DFT are provided by Hesselmann [19], but do not include the large complexes of pyrazine dimmer and 2-pyridoxine·2-aminopyridine. Note that $\Delta E_{disp} = E^{(2)}_{disp} + E^{(2)}_{exch-disp}$ in SAPT-DFT method. The X-axis coordinate represented a series of complexes in mixed subset in S22. For more details see Table 1

assessed for hydrogen bond, dispersion dominated and mixed subsets. In terms of the noncovalent interaction energies in quantitative calculation as well as their ΔE_{elstat} and ΔE_{disp} in qualitative analysis, we recommend the combination of the EDA+BLYP-D3/TZ2P, which gives the best reproduction of CCSD(T)/CBS energies and good reasonable values of ΔE_{elstat} and ΔE_{disp} for the S22 set.

Examples of intermolecular interactions

Encouraged by the satisfactory performance of EDA together with BLYP-D3/TZ2P in reasonably describing energy components and in accurately calculating interaction energies in various types of complexes, we further apply this approach to two representative large-system complexes in order to get a better insight into the binding characteristics. Porphine dimers and concave-convex complexes involving C60 are chosen for study, whose large π-systems represent difficulties for their important dispersion to be accounted correctly by general QM methods. We believe that this approach (EDA+DFT-D3/TZ2P) is a rational and alternative way to compute these complexes.

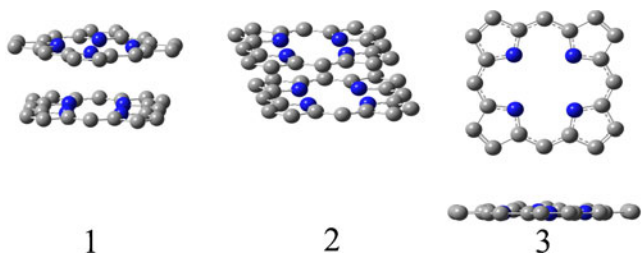

Fig. 5 Structures of porphine dimers 1~3 optimized at the B97D/TZV (2df,2dp) level (atom H is not shown); These structures were obtained from ref [49]

Porphine dimers

Porphine dimers are among the most important polar aromatic molecules not only due to their biological functions, but also their outstanding spectroscopic and photophysical properties [53–56]. Especially, the so-called π-π stacking between porphine monomer units is often believed as dispersion dominated interactions that have significant influence on structure formation and properties [49].

Although much is known about the physical and chemical properties of free porphine and its metal complexes [57], only a few reports are available about the intermolecular interaction of the dimer without a central metal atom. Various dimer structures like parallel displaced and T-shaped structures are found in solid state and have also been investigated [49]. Figure 5 sketches the representative orientation of three porphine dimers. Herein, the total interaction energies and their

Table 4 Total noncovalent interaction energies ΔE_{int} and their energy components by EDA at BLYP-D3/TZ2P for porphine dimers 1~3 (in kcal mol^{-1})

	ΔE_{int}	ΔE_{disp}	ΔE_{elstat}	ΔE_{orb}	ΔE_{pauli}	ΔE_{int} [a)]
1	−20.75	−37.70	−12.53	−3.06	32.54	−22.10
2	−22.37	−41.03	−17.16	−6.21	42.03	−25.00
3	−9.60	−11.93	−4.73	−3.49	10.55	−10.30

a) Calculated at the B2PLYP-D at TZV(2df, 2dp)level from ref [49]

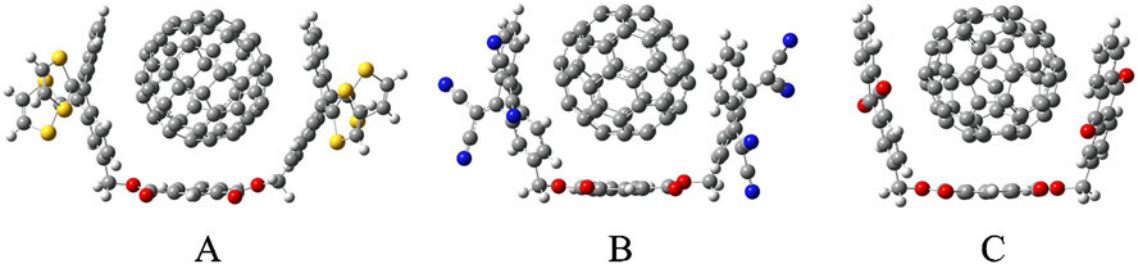

Fig. 6 Structures of concave-convex complexes involving C60 A~C optimized at the B97D/6-31+g(d,p) level

component are calculated using the EDA method together with BLYP-D3/TZ2P, which are based on the optimized geometries at the B97D/TZV(2df,2dp) level provided by Mück-Lichtenfeld [49]. The total interaction energies resulted from EDA+BLYP-D3/TZ2P are much closer to the value from B2PLYP-D (see Table 4), while the latter is believed to be a more accurate theoretical method for noncovalent interactions but more costly computationally. As demonstrated by EDA analysis, it is not surprising to observe that the dispersion contributions are absolutely essential and important for the binding of all investigated structures of porphine dimers, which reflects the stabilization of these clusters is dominated by dispersion attraction contribution. The same cases were observed by another EDA method in ref [49]. Meanwhile, the dimers of sandwich and parallel-displaced have much stronger binding strengths than that of T-shaped for the latter has smaller van der Waals interactions. Similar findings were also noted in polycyclic aromatic systems [58]. This observation is different compared with that from benzene dimers of small size π-electronic systems [59], which showed the benzene dimers of T-shaped and parallel-displaced have much stronger binding strengths than the sandwich.

Concave–convex complexes involving C60

The supramolecular complex of concave-convex type involving C60 continues to be a very active area of research [60–64], with their construction of self-organized electro-active nanostructures as main driving forces. The interactions in these concave-convex complexes are unusual because the π orbitals between curved aromatic hosts and guests are both highly polarized, which suggests that these interactions might play a distinct role in the stabilization of the complexes [63–65]. However, the nature of these types of interactions has not been clearly answered. There is a need to estimate the binding energies and their energy component contribution by reliable methods. In this work, the three complexes are optimized at B97D/6-31+g(d,p) theory of level, performing on the Gaussian 09 suite [66] (see Fig. 6). Shown in Table 5 and Fig. 6, the varied trends of the binding constants K_a from ^{1}H NMR experiment [62] are in accord with those of the total interaction energy from this approach of EDA+BLYP-D3/TZ2P, increasing in the order of C<B<A. Unfortunately, in this case, the exact noncovalent interaction compared with the experiment is not obtained by this approach. This may be attributed to the fact that the calculations are performed in the gas phase without taking into account solvent effects. The EDA results show that the binding energy has more contribution from dispersion energy ΔE_{disp} and less from electrostatic energy ΔE_{elstat}. While the orbital interaction ΔE_{orb} has few contributions to the stability of the complexes because the π orbitals do not overlap with each other well between the curved surfaces. These EDA results give us confidence in the validity of the conclusion that the electrostatic and the dispersion force are substantially operative on these systems.

Conclusions

The performance of EDA method with four types of DFT-D3 GGA-functionals (BP86-D3, BLYP-D3, PBE-D3 and SSB-D3) with three STO basis sets (DZP,TZ2P and QZ4P) is tested against the benchmark set S22. Overall, the EDA method at BLYP-D3/TZ2P level yields noncovalent interaction energies that are very close to the best CCSD(T)/CBS reference data, and there is distinct advantage in providing reasonable corresponding energy components. Thus, the EDA method at BLYP-D3/TZ2P level is a rational choice for treating the noncovalent interaction systems (particularly when involving the dispersion force), not only in terms of accuracy but also of computational cost. We therefore recommend it to the treatment of larger unsaturated systems. Two cases of large unsaturated systems, namely porphine

Table 5 Total noncovalent interaction energies ΔE_{int} and their energy components by EDA at BLYP-D3/TZ2P for the concave-convex complex A~C involving C60 (in kcal mol^{-1})

	ΔE_{int}	ΔE_{disp}	ΔE_{elstat}	ΔE_{orb}	ΔE_{pauli}	K_a/M^{-1} a)
A	−35.48	−64.93	−28.90	−14.68	73.03	3000±120
B	−33.92	−65.17	−27.68	−13.21	72.14	1540±150
C	−30.39	−57.44	−22.69	−11.31	61.05	790±50

a) Binding constant K_a/M^{-1} by ^{1}H NMR from ref [62]

dimers and concave-convex complexes involving C60, are considered here. In these two selected cases, we partition the interaction energies into the most relevant contributions from dispersion, electrostatics and orbital in order to provide qualitative insights into the binding characteristics. Further investigations into more types of functionals of DFT-D3 are currently being carried out in our group.

Acknowledgments Financial support by the National Natural Science Foundation of China (No. 21173069) is acknowledged. We are grateful to Dr. Andreas Hesselmann at Lehrstuhl für Theoretische Chemie, Universität Erlangen-Nürnberg for his results of SAPT-DFT calculation. Authors would also like to thank Prof. Christian Mück-lichtenfeld at Organisch-Chemisches Institut der Universität Münster for his structure of porphine dimers. The computation of the Gaussian is supported by the School of Chemical and Environmental Sciences, Henan Normal University.

References

1. Prins LJ, Scrimin P (2009) Angew Chem Int Ed 48:2288–2306
2. Dunitz JD, Gavezzotti A (2009) Chem Soc Rev 38:2622–2633
3. Černý J, Hobza P (2007) Phys Chem Chem Phys 9:5291–5303
4. Lein M, Frenking G (2005) The nature of the chemical bond in the light of an energy decomposition analysis. In: Dykstra CF, Frenking G, Kim KS, Scuseria GE (eds) Theory and applications of computational chemistry: the first forty years. Elsevier, Amsterdam, pp 291–372
5. Hopffgarten MV, Frenking G (2012) WIREs Comput Mol Sci 2:43–62
6. Mo Y, Bao P, Gao J (2011) Phys Chem Chem Phys 13:6760–6775
7. Su P, Li H (2009) J Chem Phys 131:014102
8. Reinhardt P, Piquemal JP, Savin A (2008) J Chem Theor Comput 4:2020–2029
9. Mitoraj MP, Michalak A, Ziegler T (2009) J Chem Theor Comput 5:962–975
10. Vyboishchikov SF, Krapp A, Frenking G (2008) J Chem Phys 129:144111
11. Cybulski H, Sadlej J (2008) J Chem Theor Comput 4:892–897
12. Rajchel Ł, Zuchowski PS, Szczesniak MM, Chałasinski G (2010) Phys Rev Lett 104:163001
13. Szalewicz K (2012) WIREs Comput Mol Sci 2:254–272
14. Jeziorski B, Moszynski R, Szalewicz K (1994) Chem Rev 94:1887–1930
15. Hohenstein EG, Sherrill CD (2010) J Chem Phys 133:014101
16. Morokuma K (1971) J Chem Phys 55:1236–1244
17. Morokuma K (1977) Acc Chem Res 10:294–300
18. Ziegler T, Rauk A (1977) Theor Chim Acta 46:1–10
19. Hesselmann A (2012) J Phys Chem A 115:11321–11330
20. Jurečka P, Šponer J, Černý J, Hobza P (2006) Phys Chem Chem Phys 8:1985–1993
21. Pitoňák M, Neogrády P, Černý J, Grimme S, Hobza P (2009) Chem Phys Chem 10:282–289
22. Marshall MS, Sears JS, Burns LA, Brédas JL, Sherrill CD (2010) J Chem Theory Comput 6:3681–3687
23. Pitoňák M, Řezáč J, Hobza P (2010) Phys Chem Chem Phys 12:9611–9614
24. Riley KE, Pitoňák M, Jurečka P, Hobza P (2010) Chem Rev 110:5023–5063
25. Pavlov A, Mitrasinovic PM (2010) Curr Org Chem 14:129–137
26. Sherrill CD (2009) Computations of Noncovalent π Interactionsin In: Lipkowitz KB, Cundari TR (Eds) Reviews in computational chemistry, vol 26, Wiley, New York, pp 1-38
27. Zhao Y, Schultz NE, Truhlar DG (2006) J Chem Theory Comput 2:364–382
28. Zhao Y, Truhlar DG (2008) Theor Chem Acc 120:215–241
29. Grimme S (2006) J Comp Chem 27:1787–1799
30. von Lilienfeld OA, Tavernelli I, Rothlisberger U (2004) Phys Rev Lett 93:153004
31. Grimme S (2006) J Chem Phys 124:034108
32. Grimme S (2011) WIREs Comput Mol Sci 1:211–228
33. Grimme S, Antony J, Ehrlich S, Krieg H (2010) J Chem Phys 132:154104
34. dftd3 program, see http://toc.uni-muenster.de/DFTD3/
35. Takatani T, Hohenstein EG, Malagoli M, Marshall MS, Sherrill CD (2010) J Chem Phys 132:144104
36. Riley KE, Pitoňák M, Černý J, Hobza P (2010) J Chem Theory Comput 6:66–80
37. van Lenthe E, Baerends EJ (2003) J Comput Chem 24:1142–1156
38. Weigend F, Ahlrichs R (2005) Phys Chem Chem Phys 7:3297–3305
39. Güell M, Luis JM, Solà M, Swart M (2008) J Phys Chem A 112:6384–6391
40. Burns LA, Vázquez-Mayagoitia Á, Sumpter BG, Sherrill CD (2011) J Chem Phys 134:084107
41. Grimme S, Antony J, Schwabe T, Mück-Lichtenfeld C (2007) Org Biomol Chem 5:741–758
42. Goerigk L, Grimme S (2011) Phys Chem Chem Phys 13:6670–6688
43. Peverati R, Baldridge KK (2008) J Chem Theory Comput 4:2030–2048
44. Thanthiriwatte KS, Hohenstein EG, Burns LA, Sherrill CD (2011) J Chem Theory Comput 7:88–96
45. Hohenstein EG, Chill ST, Sherrill CD (2008) J Chem Theory Comput 4:1996–2000
46. Korth M, Thiel W (2011) J Chem Theory Comput 7:2929–2936
47. Goerigk L, Grimme S (2010) J Chem Theory Comput 6:107–126
48. Safonov AA, Rykova EA, Bagaturyants AA, Sazhnikov VA, Alfimov MV (2011) J Mol Model 17:1855–1862
49. Mück-Lichtenfeld C, Grimme S (2007) Mol Phys 105:2793–2798
50. Baerends EJ, Autschbach J, Bashford D, Bérces A, Bickelhaupt FM, Bo C, Boerrigter PM, Cavallo L, Chong DP, Deng L, Dickson RM, Ellis DE, van Faassen M, Fan L, Fischer TH, Fonseca Guerra C, Ghysels A, Giammona A, van Gisbergen SJA, Götz AW, Groeneveld JA, Gritsenko OV, Grüning M, Harris FE, van den Hoek P, Jacob CR, Jacobsen H, Jensen L, van Kessel G, Kootstra F, Krykunov MV, van Lenthe E, McCormack DA, Michalak A, Mitoraj M, Neugebauer J, Nicu VP, Noodleman L, Osinga VP, Patchkovskii S, Philipsen PHT, Post D, Pye CC, Ravenek W, Rodríguez JI, Ros P, Schipper PRT, Schreckenbach G, Seth M, Snijders JG, Solà M, Swart M, Swerhone D, te Velde G, Vernooijs P, Versluis L, Visscher L, Visser O, Wang F, Wesolowski TA, van Wezenbeek EM, Wiesenekker G, Wolff SK, Woo TK, Yakovlev AL, Ziegler T (2012) ADF version 2012.01, SCM, Theoretical Chemistry. Vrije Universiteit, Amsterdam, http://www.scm.com
51. Grimme S, Ehrlich S, Goerigk L (2011) J Comput Chem 32:1456–1465
52. Riley KE, Hobza P (2008) J Chem Theory Comput 4:232–242
53. Ohira S, Brédas J-L (2009) J Mater Chem 19:7545–7550
54. Ahn TK, Kim KS, Kim DY, Noh SB, Aratani N, Ikeda C, Osuka A, Kim D (2006) J Am Chem Soc 128:1700–1704
55. Aittala PJ, Cramariuc O, Hukka TI (2011) Chem Phys Lett 501:226–231
56. Day PN, Nguyen KA, Pachter R (2008) J Chem Theory Comput 4:1094–1106
57. Yang Q-Z, Khvostichenko D, Atkinson JD, Boulatov R (2008) Chem Commun 38:963–965
58. Podeszwa R, Szalewicz K (2008) Phys Chem Chem Phys 10:2735–2746
59. Hohenstein EG, Sherrill CD (2009) J Phys Chem A 113:878–886

60. Gayathri SS, Wielopolski M, Pérez EM, Fernández G, Sánchez L, Viruela R, Ortí E, Guldi DM, Martín N (2009) Angew Chem Int Ed 48:815–819
61. González-Rodríguez D, Carbonell E, Guldi DM, Torres T (2009) Angew Chem Int Ed 48:8032–8036
62. Pérez EM, Capodilupo AL, Fernández G, Sánchez L, Viruela PM, Viruela R, Ortí E, Bietti M, Martín N (2008) Chem Commun 38:4567–4569
63. Pérez EM, Martín N (2008) Chem Soc Rev 37:1512–1519
64. Kawase T, Kurata H (2006) Chem Rev 106:5250–5273
65. Wong BM (2009) J Comput Chem 30:51–56
66. Frisch MJ, Trucks GW, Schlegel HB, Scuseria GE, Robb MA, Cheeseman JR, Scalmani G, Barone V, Mennucci B, Petersson GA, Nakatsuji H, Caricato M, Li X, Hratchian HP, Izmaylov AF, Bloino J, Zheng G, Sonnenberg JL, Hada M, Ehara M, Toyota K, Fukuda R, Hasegawa J, Ishida M, Nakajima T, Honda Y, Kitao O, Nakai H, Vreven T, Montgomery JA Jr, Peralta JE, Ogliaro F, Bearpark M, Heyd JJ, Brothers E, Kudin KN, Staroverov VN, Kobayashi R, Normand J, Raghavachari K, Rendell A, Burant JC, Iyengar SS, Tomasi J, Cossi M, Rega N, Millam JM, Klene M, Knox JE, Cross JB, Bakken V, Adamo C, Jaramillo J, Gomperts R, Stratmann RE, Yazyev O, Austin AJ, Cammi R, Pomelli C, Ochterski JW, Martin RL, Morokuma K, Zakrzewski VG, Voth GA, Salvador P, Dannenberg JJ, Dapprich S, Daniels AD, Farkas O, Foresman JB, Ortiz JV, Cioslowski J, Fox DJ (2010) Gaussian 09 C01. Gaussian Inc, Wallingford, CT